Simulation of the Electromagnetic Flux Compression using LS-DYNA® Multi-Physics Capability

Kunio Takekoshi

Terrabyte Co., Ltd, NOV BLDG 3F, 3-10-7, Yushima, Bunkyo-ku, Tokyo, 113-0034, Japan

1 Introduction

When a time-varying magnetic field is given to electrically conductive materials, induced electric current is emerged on the surface of the materials, and then the material is deformed by Lorentz force emerged from the magnetic field and the induced electric current. This is a simple principle of electro-magnetic forming technique.

It has been challenging to numerically predict shape of an electrically conductive object deformed by the electro-magnetic forming technique, because the electro-magnetic forming process involves large deformation of material, hi-speed deformation process, and thermal effect to material properties by joule heating due to induced electric current.

Since the release of version R.7.0, LS-DYNA can simulate electromagnetism behavior. In combination with the electromagnetism solver and established/sophisticated structural and thermal solvers, LS-DYNA can simulate the electro-magnetic forming process using one FEM model within one code without any extra licenses.

In this study, simulation results for the electro-magnetic compression method are presented. The method employs the electro-magnetic forming technique and has been experimentally investigated by a lot of researchers for a long time since 1960s. Thus the simulation of the electro-magnetic flux compression can be a good benchmark test for LS-DYNA multi-physics capability.

2 The Electro-Magnetic Flux Compression

2.1 Purpose, Principle and Experimental Procedure

The electro-magnetic flux compression is mainly used to investigate electronic property of materials such as Carbon Nano Tubes and is also used to prove theories developed in the condensed matter physics and the statistical physics. This is because the spin and the orbital motion of electrons are affected and precisely controlled by magnetic flux density.

A schematic illustration of the electro-magnetic flux compression system is shown in Fig.1. This is based on the system which has been developed by the International Megagauss Science Laboratory, the ISSP, University of Tokyo [1-3]. There are 4 components, a liner coil, a primary coil, a support coil, and a Helmholtz coil in the system. The liner and primary coils are made of bulk copper (or can be represented as a single turn copper coil). The support coil is made of bulk steel (a single turn steel coil). The Helmholtz coil is composed of two coils (242 turns for each coil) using copper wire.

A specimen of interest is placed at the center of the liner coil during experiment with pickup coils to measure magnetic field, and its temperature is usually controlled using a cryostat. The specimen placed at the system developed by the ISSP-group is subjected to ultra-high magnetic flux density nearly 730 T [1].

The experimental procedure is as follows;

- 1. The external seed field is developed from 0 to certain value within several ten milliseconds using the Helmholtz coil. The direction of the electric current $I_{\mathrm{H.}}$ injected into the Helmholtz coil is depicted in Fig.1(a). The direction of the seed field $B_{\mathrm{ext.}}$ is also depicted along the coil axis.
- 2. After the achievement of the certain value of the seed field, the primary and support coils are driven to emerge induced electric current on the surface of the liner coil. The direction of the electric current $I_{\mathrm{P.}}$ injected into primary and support coils is shown by the arrow depicted in the Fig.1(a).
- 3. The liner coil is imploded by the Lorentz repulsion force between the linear and primary coils. The typical period of the implosion of the liner coil is about 40 microseconds.
- 4. The induced current in the liner mainly generates ultra-high magnetic flux density (several hundred Tesla) in the center of the liner coil. The direction of the ultra-high magnetic field is the same as that of the external seed field.

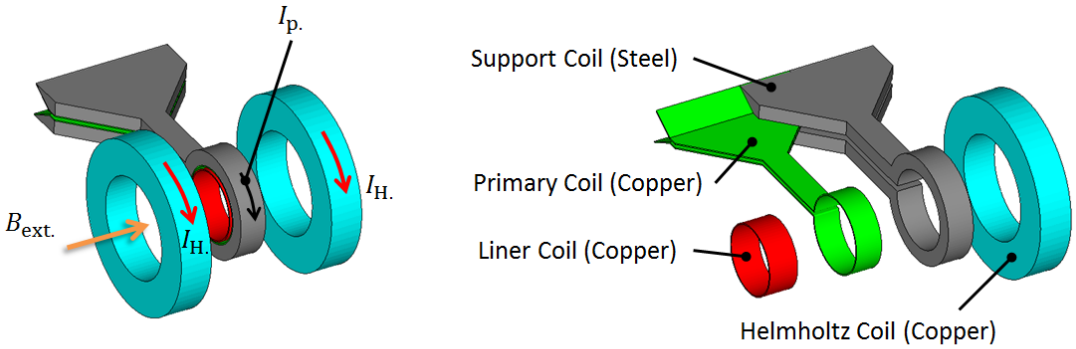

(a) An apparatus of the EMFC (b) Exploded view

Fig.1: The electro-magnetic flux compression (EMFC) system developed by the ISSP [1-3].

2.2 Simulation

2.2.1 LS-DYNA and Computer Environment

In this study, development version of MPP-DYNA (SVN Revision 95378) is employed to invoke a feature of the electromagnetism solver. The feature is mentioned in the section of "Recalculation Cycle of BEM and FEM Matrices".

The development version of MPP-DYNA has been executed on a cluster environment with four compute nodes and a login node connected each other using Infini-band FDR-10 (40Gbps) network system. CPUs and main memory mounted on the each compute node are two Intel Xeon E5-2680 (2.70GHz – 3.5GHz) and 64GBytes, respectively. Operating system of the cluster nodes are CentOS 6.3 64bit.

Sixteen cores out of sixty-four cores are employed to execute MPP-DYNA in this study. Elapsed time for a simulation model used in this study is more than 30 hours, depending on control parameters of LS-DYNA and CPU's clock up feature provided by Turbo-Boost mechanism of Intel CPUs.

2.2.2 Finite Element Model

A simulation model used in this study is shown in Fig. 2. The model includes 102,454 nodes and 88,612 finite elements. The primary and support coils are connected using nodal equivalence, not electric contact condition. All of the elements in this study are hexahedral elements with one point integration (default formulation), and thickness of elements on the surface of the liner coil is thin (0.2 mm) so that eddy current problem can be precisely predicted. Elements of the Helmholtz coil are almost uniform, because the Helmholtz coil is composed of two 242-turns coils and electric current in the coil is uniform. This model is able to be commonly used in structural, thermal and electro-magnetic analyses.

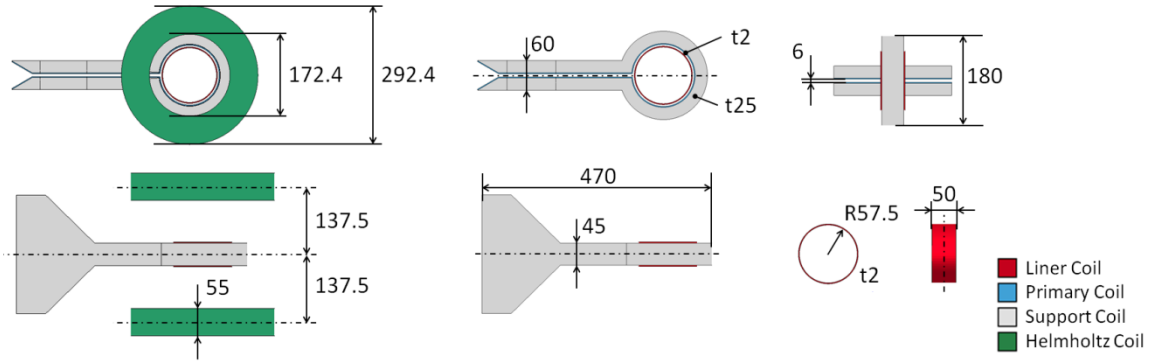

Fig.2: A simulation model of the electro-magnetic flux compression system used in this study. The unit used in this figure is mm.

2.2.3 Boundary Conditions

All parts are constraint using SPC condition during *Phase 1* analysis, and surfaces of the left-end of primary and support coils are also constraint using SPC condition during *Phase 2* analysis. The latter constraint condition corresponds to the clamp of the electrodes directly connected to the primary and support coils. SPC Condition during *Phase 2* analysis is shown in Fig.3.

Initial temperature for whole model is set to 298.15 K, because measurements using the electro-magnetic flux compression are usually carried out in room temperature environment.

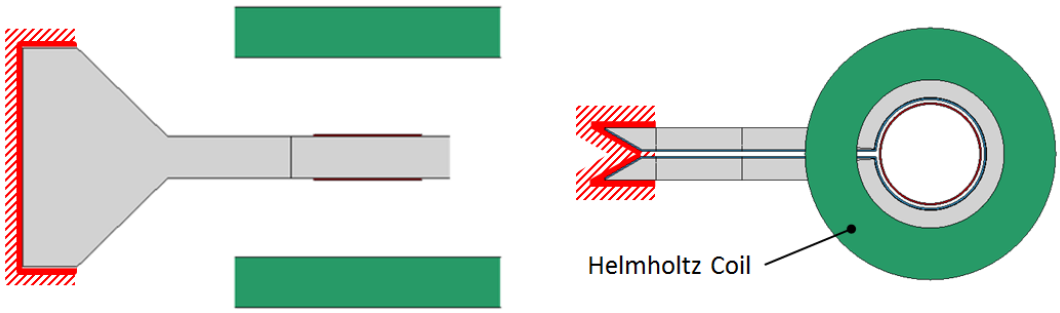

Fig.3: SPC boundary conditions in Phase 2 analysis. The Helmholtz coil is completely constraint in Phase 1 and 2 analyses.

2.2.4 Electric current Setup

Time history of electric current injected into the Helmholtz coil is shown in Fig.4 and is considered using a keyword **`*EM_CIRCUIT_SOURCE`** to represent solenoid coil. The electric current in the Helmholtz coil gradually increases using a STEP function invoked by **`*DEFINE_CURVE_FUNCTION`** and finally achieves 0.0155 (MA) per 1 coil turn, and then continues constantly flowing until the end of electro-magnetic flux compression process.

Time history of electric current injected into the primary and support coils is shown Fig.5 and is considered using a keyword **`*EM_CIRCUIT`**, because these coils are single turn bulk coils and the skin effect of eddy current has to be considered. The data was obtained from ref. [2] with a digitizer program.

Development of the external seed field takes 20 milliseconds to achieve 3.8 Tesla in experiments [4]. After the achievement, the procedure of the electro-magnetic flux compression starts. The period of the electro-magnetic flux compression measurement is 50 microseconds which is much smaller than that of the development of the external seed field. In this study, the period for the development of the external seed field is defined as *Phase 1* from 0 to 20 (msec), and the period for the electro-magnetic flux compression measurement is defined as *Phase 2* which starts from 20 (msec) and ends at 20.050 (msec).

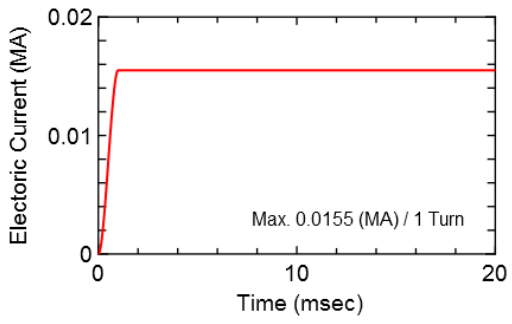

Fig.4: Time history of electric current injected into the Helmholtz coil.

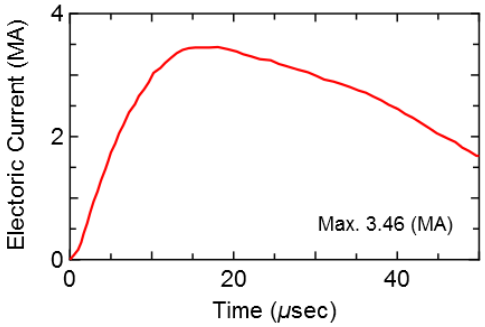

Fig.5: Time history of electric current injected into the primary and support coils.

2.2.5 Constitutive Material Models and Its Parameters

Materials for the components and corresponding constitutive model for the materials used in the structural solver are listed in table.1. The liner and primary coils are modelled using tabulated Johnson-Cook model (***MAT_224**) which can consider temperature dependent Young's modulus. The support and the Helmholtz coils are modelled using Johnson-Cook model (***MAT_015**) and rigid model (***MAT_020**), respectively, because the support and Helmholtz coils are not of interest in this study.

Equation of state is also considered using ***EOS_GRUNEISEN** for the liner, primary and support coils. Its constants are determined by reference [5, 6].

Material constants used by electromagnetism solver are determined by references [7] for copper, and by references [8] for steel. In this study, temperature dependence of electrical conductivities for liner (copper), primary coil (copper) and support coil (steel) are considered using ***EM_MAT_001** and ***EM_EOS_TABULATED1**.

Material constants used by thermal solver are determined by references [5, 9] for copper, and by references [6, 9] for steel. In this study, temperature dependence of thermal conductivity and specific heat for liner (copper), primary coil (copper) and support coil (steel) are considered using ***MAT_THERMAL_ISOTROPIC_TD_LC**.

Table 1: Components, material, and corresponding constitutive model in this study.

Component	Material	Constitutive model	EOS	Constants
Liner Coil	Copper	Johnson-Cook [10]	Gruneisen	Ref. [5, 11]
Primary Coil	Copper	Johnson-Cook	Gruneisen	Ref. [5, 11]
Support Coil	Steel	Johnson-Cook	Gruneisen	Ref. [6]
Helmholtz Coil	Copper	Rigid	N/A	N/A

2.2.6 Time Step Size Control

Time step control is important in analyzing the electro-magnetic flux compression, because velocity of deformation of the liner coil was estimated to be 2.4 km/sec in experiments [1]. In this study, scale factor for computed time step is set to 0.67, the value for high explosive analysis. Computed time step size for the considered model is about 2.0e-8 (sec) or larger in *Phase 2* analysis.

Time step size considered by the thermal solver used in this study is set using LCTS of ***CONTROL_THERMAL_TIMESTEP**, time history of thermal time step size. In *Phase 1* analysis, time step size gradually decreases from 1.0e-05 to 1.0e-07 (sec). In *Phase 2* analysis, time step size is fixed at 1.0e-07 (sec), five times larger than that computed by structural solver.

Time step size considered by the electromagnetism solver used in this study can be automatically computed based on the diffusion equation for the magnetic field [12], and this automatic time step control is invoked using ***EM_CONTROL_TIMESTEP** where TSTYPE is set to 1. FACTOR for the keyword in this study is set to 1.0. In *Phase 1* analysis, electromagnetism time step size is 1.3e-06 (sec), while in *Phase 2* analysis, the time step size decreases from 1.3e-06 to 1.2e-07 (sec).

2.2.7 Recalculation Cycle of BEM and FEM Matrices

In the electromagnetism solver of LS-DYNA, BEM matrices have to be recalculated when conductor parts are moved, or are deformed, because the BEM matrices depend on the surface node coordinates of the conductors [12]. FEM matrices in the electromagnetism solver also have to be recalculated when conductor parts are deformed, or material properties considered by the electromagnetism solver are changed. Recalculation cycle for BEM and FEM matrices can be set using NCYCLEBEM of ***EM_SOLVER_BEM** and NCYCLEFEM of ***EM_SOLVER_FEM**, respectively.

It is important to reduce unnecessary recalculation cycle, because it takes more than 5 minutes to carry out 1 recalculation cycle in the model shown in Fig.2. In *Phase* 1 analysis, since all conductors are fully constraint, setting the cycle to a large value is justified. However, in *Phase* 2 analysis, since the electro-magnetic forming is considered, the recalculation cycle has to be set to 1. Since constant recalculation cycle can be set in the official version of LS-DYNA / MPP-DYNA solvers, there is no choice in setting the recalculation cycle to 1 in order to obtain an appropriate simulation result in this study. If the recalculation cycle is set to 1 in *Phase* 1 and 2 analyses, the number of recalculation is about 16,000, and it takes more than 56 days to analyze the electro-magnetic flux compression, which means unrealistic solution.

The development version of MPP-DYNA (SVN Revision 95378) can consider the recalculation cycle as a function of time. Setup of the recalculation cycle considered in this study is shown in Fig. 6 and Fig. 7. In *Phase 1* analysis, the cycle gradually decreases from the default value (5000 steps provided by the solver) to 1 step, because all conductors are fully constraint and temperature change is negligible. In *Phase 2* analysis, the cycle is always set to 1, because liner, primary, and support coils are drastically deformed by electro-magnetic forming technique and temperature change in these coils are large from room temperature to melting point, for example. With this setup, it takes about 2 days to analyze the electro-magnetic flux compression.

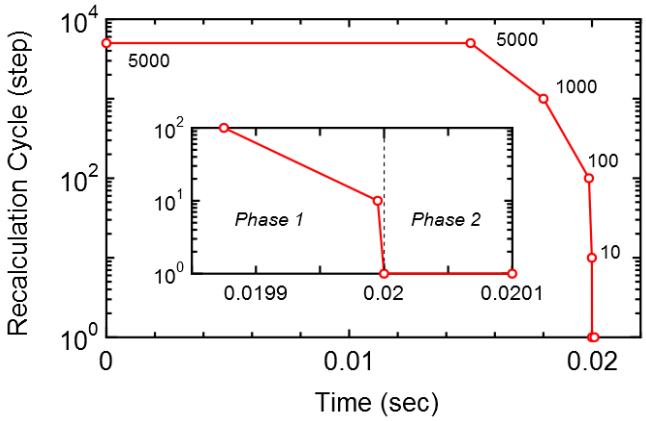

Fig.6: Recalculation cycle as a function of time used in this study. Inset also shows the recalculation cycle used in Phase 2 analysis.

```
*EM_SOLVER_BEM
$    RELTOL     MAXITE      STYPE     PRECON     USELAS NCYCLEBEM
     1.e-6        1000          2          2          1    -12345
*EM_SOLVER_FEM
$    RELTOL     MAXITE      STYPE     PRECON     USELAS NCYCLEFEM
     1.e-3        1000          1          1          1    -12345
*DEFINE_CURVE_TITLE
NcycleBEM, NcycleFEM
$      LCID      SIDR       SFA       SFO      OFFA      OFFO
     12345
              0.000000                5000
              0.015000                5000
              0.018000                1000
              0.019875                 100
              0.019995                  10
              0.020000                  10
              0.020100                   1
$
```

Fig.7: Input keyword to tweak NCYCLEBEM and NCYCLEFEM. Negative value of NCYCLEBEM/FEM can activate the recalculation cycle of BEM/FEM matrices as a function of time. This feature is available in the development version of MPP-DYNA, SVN revision 95378.

2.2.8 Output Data Setup

Magnetic flux density at certain position can be evaluated using **`*EM_DATABASE_POINOUT`** and **`*LSO_DOMAIN`** keywords. Positions to evaluate magnetic flux density in this study are shown in Fig. 8. In this study, the former keyword is used during *Phase 1* analysis to output magnetic flux density at each position every 5.0e-04 sec, the latter one is used during *Phase 2* analysis to output them at the same position every 2.0e-07 sec.

The output of magnetic flux density requires much calculation cost, and it is roughly estimated to be one minute in this study. Thus, it is also important to reduce output cycle and output location.

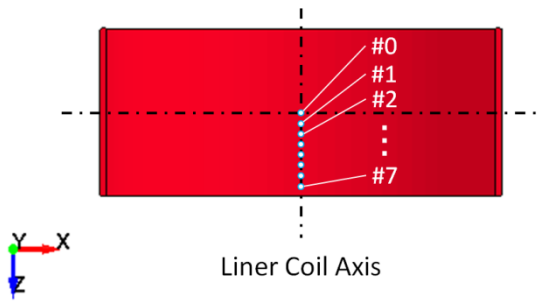

Position	X	Y	Z
#0	0.0	0.0	0.0
#1	0.0	0.0	3.1
#2	0.0	0.0	6.8
#3	0.0	0.0	9.7
#4	0.0	0.0	12.0
#5	0.0	0.0	16.0
#6	0.0	0.0	19.0
#7	0.0	0.0	22.0

Fig.8: Positions of pickup coils to measure magnetic field, from #0 to #7. Figures used in the above table show coordinate value of pickup coils (unit : mm).

3 Results

3.1 Phase1: External Seed Field

Time history of the external seed field at the location of the pickup coil #0 is shown in Fig. 9 (Left). At 20 (msec), the value of the external seed field is about 3.8 (T). Although the injected electric current into the Helmholtz coil is almost the constant as shown in Fig. 4, the seed field gradually increases due to induced electric current in the liner and other coils.

Contour plot of temperature for the system of the electro-magnetic flux compression is shown in Fig. 9 (Right). Twelve K increase is observed in the liner coil due to the Joule heating effect by the induced electric current on the surface of the liner coil.

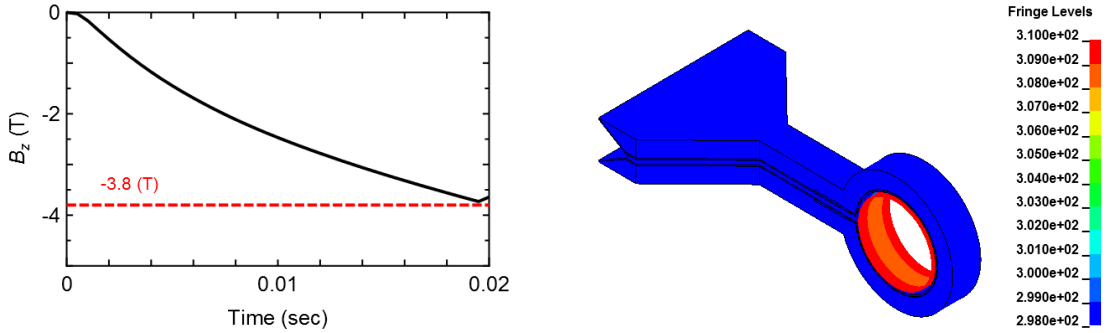

Fig.9: (Left) Time history of the external seed field along the coil axis. (Right) Contour plot of temperature for the system of the electro-magnetic flux compression at 20 msec.

3.2 Phase2: Electro-Magnetic Flux Compression

The electro-magnetic flux compression simulation has been carried out until 20.047 milliseconds, and is terminated by MF2 Initialization error. Thus, the simulation result until 20.047 milliseconds is presented and discussed with an experimental result reported by ref. [3] which has been freely accessed. Elapsed time of the simulation result shown below is subtracted 20.0 milliseconds from the simulation time, ranging from 0 microsecond to 47 microseconds.

3.2.1 Magnetic Flux Density

Spatial dependence of magnetic flux density (intensity) at different times obtained by an experiment and the simulation studied is shown in Fig.10. Open and close circles are evaluated at the positions listed in Fig. 8. It is found that the experimental data obtained at 38.7, 38.2, 37.7 and 37.2 microseconds roughly correspond to the simulation data obtained at 47.0, 46.3, 45.8 and 45.2 microseconds, respectively, on the basis of the maximum value of magnetic flux density Bz. It is also

found that the feature of double peak emearging around 10 mm and growing with time proceeding is predicted in the simulation result like the experimental result.

Time history of compressed magnetic flux density measured at the position #0 is shown in FIg.11. In Fig.11 (a) The data obtained by the experiment [3, 13] and the simulation are directory compared, showing the difference between them. As shown in FIg.11 (b), by normalizing time data of the simulation result with the factor 0.823 (= 38.7 / 47.0) shown in Fig.10, the data obtained by the simulation is found to show good agreement with the experimental result.

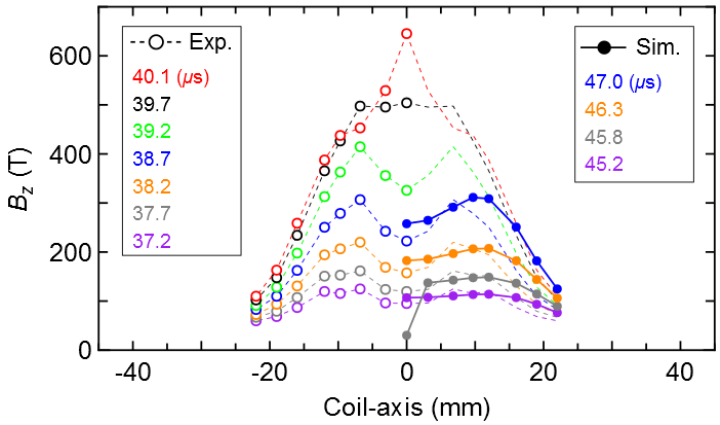

Fig.10: Spatial dependence of magnetic flux density (intensity) at different times obtained by an experiment (open circle with dashed line) [3, 13] and the simulation considered in this study (closed circle with solid line).

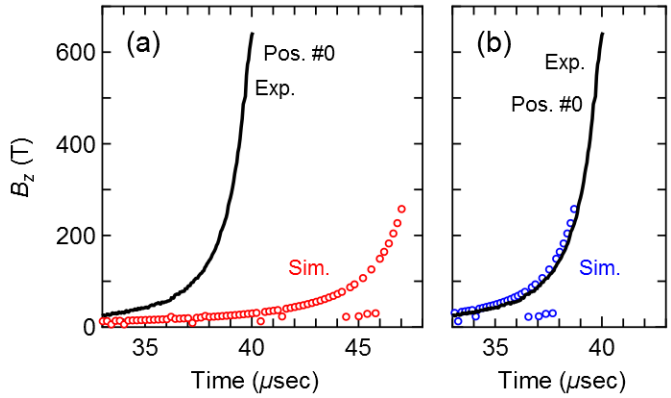

Fig.11: Time history of compressed magnetic flux density measured at position #0. (a) Raw data obtained by an experiment [3, 13] and the simulation considered in this study are compared. Some numerical noises outside of the trend of the time evolution are seen and discussed in later section. (b) Time-axis for the simulation data is normalized to fit the experimental data.

3.2.2 Deformation of the Liner Coil

Time evolution of the liner coil predicted by the simulation is shown in Fig. 12 (Top), and a typical time evolution of the liner coil taken by high-speed framing camera in the experiment [3] is shown in Fig.12 (Bottom). On the basis of the correspondence between the experiment and the simulation found in FIg.10, snapshots of the simulation result are chosen.

Diameter of the liner coil as a function of magnetic flux density at the location of pickup coil #0 is shown in Fig.13 (Left), and the definition of the diameter is shown in Fig.13 (Right) with an example of the simulation result obtained at 47.0 microseconds. It is found that both of the simulation and the experiment data shows the same trend less than 100 T, but more than 100 T region, the diameter for the simulation result is underestimated as compared with the experimental result. It is also found that

the minimum diameter of the liner coil observed in the simulation is roughly the same as that in the experimental result shown in Fig. 13 (Right).

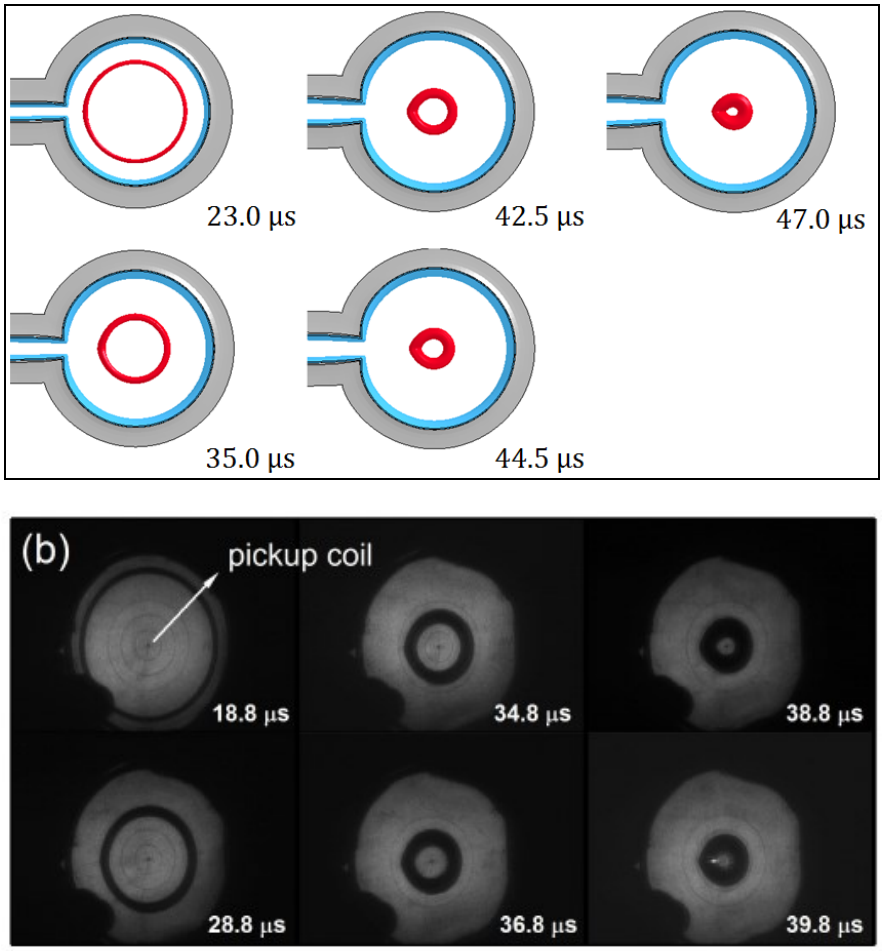

Fig.12: (Top) Evolution of liner coil predicted by the electro-magnetic flux compression simulation. (Bottom) A typical shadowgraph of the imploding liner [3, 14].

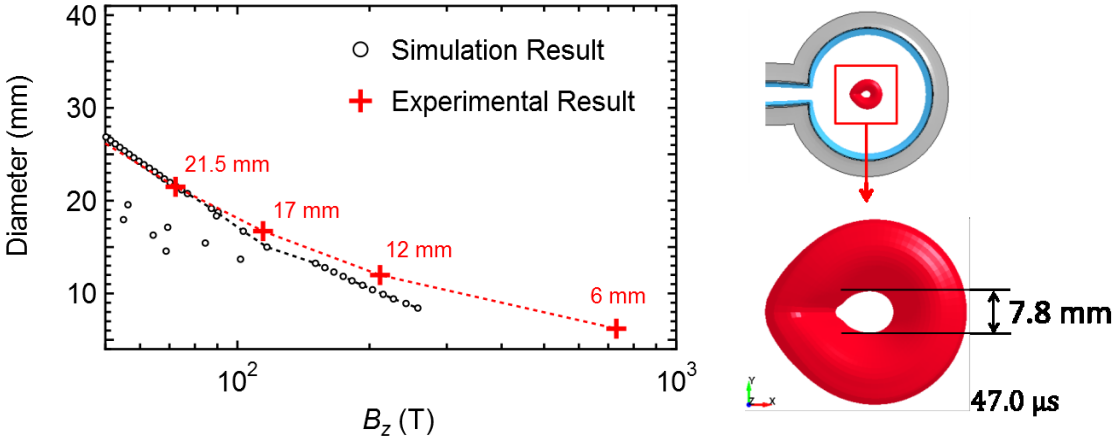

Fig.13: (Left) Diameter of the liner coil as a function of magnetic flux density at the location of pickup coil #0. The experimental result shown by red-cross and red-figure was obtained from reference [1, 15]. (Right) Diameter of the liner coil obtained by the simulation at 47.0 microseconds.

4 Discussion

From the results shown above, it is obiously found that the analysis carried out in this study can simulate a typical behavior of the electro-magnetic compression shown in figures 11, 12 and 13, but that the analysis cannot completely predict the experimental results where magnetic flux density inside the liner coil achieves more than 700 T.

From the Fig. 13, the diameter of the liner coil obtained by the simulation (7.8 mm) is almost the same as that obtained by the experiment (6 mm). However, the compressed magnetic flux density inside the liner obtained by the simulation is one third of that by the experiment. One of the reason for this contradiction is that the induced electric current flowing in the liner coil is smaller than that in the experiment. This is because the compressed magnetic field is mainly generated by the induced current in the liner coil. Moreover, the larger the induced current in the liner coil is, the larger the compressive force (Lorentz force) is. To obtain magnetic flux density more than 700 T in side the liner coil, the induced electric current in the liner has to be three times larger than that in the simulation result of this study.

Two interesting behaviors in the experimental result are shown in Fig. 10 where (1) the compressed magnetic flux density at position #0 (coil-axis is 0 mm) drastically increases from 330 T at 39.2 microseconds to 650 T at 40.1 microseconds and (2) two humps in the spatial dependence of magnetic flux density until 39.2 microseconds changes into single peak at 40.1 microseconds. One of the reasons to address the behaviors was provided by D. Nakamura et., al, the ISSP [3, 13]. They obtained two 2D-axisymmetric simulation results. One was that the center of the liner coil was compressed in advance of the edge of the coil and the single peak in the spatial dependence of magnetic flux density for the simulation was observed. The other was that the edge of the coil was compressed in advance of its center and the two humps in the spatial dependence of magnetic flux density for the simulation was observed. The simulation result presented in this paper is categorized as the latter case as shown in Fig. 14 where the width of the liner coil becomes small as compared with that of the primary coil. The difference between two reported simulation results has to be understand from the viewpoint of mechanical engineering.

An annoying point in the simulation result obtained in this study is that some numerical noise are found in evaluating magnetic flux density as shown in Fig. 11 and Fig. 13. Setting tolerance parameters of **`*EM_SOLVER_`** ten times smaller than the values by default seems to be effective, but not decisive in this simulation.

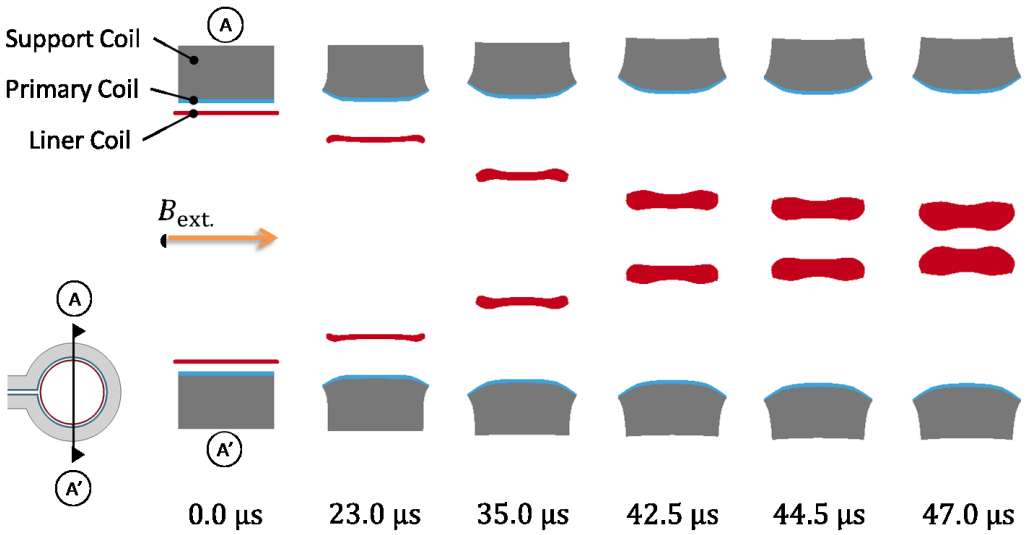

Fig.14: Time evolution of deformation of the electro-magnetic flux compression system obtained by the simulation in this study at cross section A-A'.

5 Summary

The Electro-magnetic flux compression using LS-DYNA multi-physics capability is presented. The deformation of the liner coil shown in this study is qualitatively the same as the typical experimental result reported in previous papers. Therefore LS-DYNA can be helpful tool in predicting

deformations of electrical conductive parts subjected to the elect-magnetic forming. However, the generated magnetic flux density simulated by LS-DYNA is about one third times of the value measured by experiments. More sophisticated methods and knowledge about the electromagnetic forming simulation are required to address the discrepancy of the compressed magnetic field between typical experimental results and simulation results.

6 Literature

[1] Takeyama, S. and Kojima, E., “A copper lined magnet coil with maximum field of 700 T for electromagnetic flux compression”, J. Phys. D: Appl. Phys., 44 (2011), 425003

[2] Takeyama, S., "The World Highest Magnetic Field as Indoor Generation and Its Application to Solid State Physics," The Physical Society of Japan, vol. 67, no. 3, 2012, p. 170 (in Japanese).

[3] Nakamura, D., Sawabe, H., Matsuda, Y. M., and Takeyama, S., "Dynamical Process of Liner Implosion in the Electromagnetic Flux Compression for Ultra-high Magnetic Fields," arXiv, 2013, p. 1309.1038

[4] Private communication with Professor Takeyama and Nakamura, the ISSP.

[5] Banerjee, B., "An evaluation of plastic flow stress models for the simulation of high-temperature and high-strain-rate deformation of metals," cond-mat, 2005, p. 0512466v1.

[6] Banerjee, B., “The Mechanical Threshold Stress model for various tempers of AISI 4340 steel,” cond-mat, 2005, p. 0510330v1.

[7] Matula, R. A., "Electrical Resistivity of Copper, Gold, Palladium, and Silver," J. Phys. Chem. Ref. Data, vol. 8, no. 4, 1979, p. 1147.

[8] Japan Society of Thermophysical Properties, Thermophysical Properties Handbook, YOKENDO, 2008, p. 210. (in Japanese)

[9] Powel, R. W., Ho, C. Y. and Liley, P. E., "Thermal Conductivity of Selected Materials," National Standard Reference Data Series - National Bureau of Standards - 8, 1966

[10] Johnson, G. R. and Cook, W. H. "A constitutive model and data for metals subjected to large strains, high strain rates and high temperatures.," Proc. 7th Int. Symposium on Ballistics., 1983, pp. 541-547.

[11] Ledbetter, H. M. and Naimon, E. R., "Elastic Properties of Metals and Alloys. II. Copper," J. Phys. Chem. Ref. Data, vol. 3, no. 4, 1974, pp. 897-935.

[12] Livermore Software Technology Corporation, LS-DYNA KEYWORD USER'S MANUAL VOLUME III Multi-Physics Solvers, 2015.

[13] Nakamura, D., Sawabe, H., and Takeyama, S., "Note: Experimental evidence of three-dimensional dynamics of an electromagnetically imploded liner," Review of Scientific Instruments, vol. 036102, 2014, p. 85.

[14] Photos are presented from the International Megagauss Science Laboratory, the ISSP, Univ. of Tokyo by their courtesy.

[15] Takeyama, S., Sawabe, H., and Kojima, E., "Recent Developments of the Electro-Magnetic Flux Compression," Journal of Low Temperature Physics, vol. 159, 2010, pp. 328-331.